PCCP



PAPER



Cite this: Phys. Chem. Chem. Phys., 2023, 25, 23530

Received 21st July 2023, Accepted 22nd August 2023

DOI: 10.1039/d3cp03479h

rsc.li/pccp

Heavy pnicogen atoms as electron donors in sigma-hole bonds†

Akhtam Amonov^a and Steve Scheiner **

DFT calculations evaluate the strength of σ -hole bonds formed by ZH₃ and ZMe₃ (Z = N, P, As, Sb) acting as electron donor. Bond types considered include H-bond, halogen, chalcogen, pnicogen, and tetrel bond to perfluorinated Lewis acids FH, FBr, F₂Se F₃As, F₄Ge, respectively, as well as their monofluorinated analogues. All of the Z atoms can engage in bonds of at least moderate strength, varying from 3 to more than 40 kcal mol⁻¹. In most cases, N forms the strongest bonds, but the falloff from P to Sb is quite mild. However, this pattern is not characteristic of all cases, as for example in the halogen bonds, where the heavier Z atoms are comparable to, or even stronger than N. Most of the bonds are strengthened by replacing the three H atoms of ZH₃ by methyl groups, better simulating the situation that would be generally encountered. Structural and NMR shielding data ought to facilitate the identification of these bonds within crystals or in solution.

Introduction

Not only is the H-bond (HB) the oldest of the assortment of noncovalent bonds, but this phenomenon has fostered what is perhaps the largest body of research over the last century^{1–12} This AH·B bridging interaction was originally conceived as connecting A and B atoms that are highly electronegative, viz. O, N, and F. But this definition has broadened immensely over ensuing years, to include quite a few atoms of the periodic table, many of which would not be thought of as electronegative. 13-18 The HB owes its stability in part to a certain amount of charge transfer from the base atom B to a $\sigma^*(AH)$ antibonding orbital, which leads in turn to the usual finding of a stretched A-H bond, with a lowered vibrational stretching frequency. Although the source of electrons on B was originally considered to be a lone pair, this idea has also broadened over the years. It is now recognized that the donated density may come from a π -electron cloud on the base molecule, whether localized as for acetylene, or delocalized over an aromatic phenyl ring. 19-22 Another, albeit less common, source is a σ -bonding orbital in a molecule such as H_2 .^{23,24}

One of the more interesting directions in which HB research has encompassed atoms other than the original first-row O, N,

F set is the enlargement to atoms lower in the periodic table. In the chalcogen column, for example, the heavier S, Se, and Te atoms are now all recognized to participate in HBs, as both proton donor and acceptor, in a wide range of systems spanning both chemistry and biochemistry. 14,25-29 The same can be said of the neighboring pnicogen and halogen families of elements.

A second area of growth of the HB concept is the generalization to atoms other than H. That is, the bridging proton can be replaced by any of a large set of atoms, generally drawn from the right side of the periodic table. The halogen bond, for example, may be written AX·B where X refers to Cl, Br, or I. Even though these electronegative atoms carry an overall partial negative charge within the AX molecule, they retain a small restricted area of positive potential along the extension of the AX covalent bond. This so-called σ -hole can attract a nucleophile in much the same way as the proton in the HB.30-42 The remainder of the bonding components of the HB are left essentially unchanged, i.e. the charge transfer from base to acid and dispersive attraction. This same idea extends to atoms from families other than halogen: chalcogen, pnicogen, and tetrel bonds replace the proton by atoms drawn from that particular periodic table column. 27,43-68

Just as larger atoms have been shown to participate in HBs, one might anticipate the same to be true of these other σ -hole bonds. And indeed, it has been shown that each step in the growth of the bridging atom strengthens the incipient bond. For example, I forms stronger halogen bonds than does Br, which is in turn stronger then Cl. This pattern is largely attributed to the growing polarizability and electropositivity of the larger X atom, both of which manifest as a deeper σ -hole.

^a Department of Optics and Spectroscopy Engineering Physics Institute, Samarkand State University, University blv. 15, Samarkand 140104, Uzbekistan

^b Department of Chemistry and Biochemistry, Utah State University Logan, Utah 84322-0300, USA. E-mail: steve.scheiner@usu.edu

[†] Electronic supplementary information (ESI) available: It contains deformation energies of the various complexes and unnormalized intermolecular distance, and lists the Cartesian coordinates of monomers and complexes. See DOI: https:// doi.org/10.1039/d3cp03479h

PCCP Paper

Quite unlike what has been established for the Lewis acid atom, the vast bulk of previous work has centered on base atoms drawn from the first row, i.e. F, O, and N. There is surprisingly little information concerning the capability of the larger base atoms to act as electron donors in this class of σ -hole bonds. 69-73 Given the growing consensus on their participation within HBs, this neglect leaves a large hole in our understanding of these other sorts of related bonds.

The current work represents an attempt to remedy this deficiency in the literature. The entire repertoire of σ -hole bonds is explored, encompassing halogen, chalcogen, pnicogen, and tetrel bonds, as well as HBs as a point of comparison. The Lewis acid atoms are taken from the 3rd row of the periodic table: Br, Se, As, and Ge, which ought to provide deep enough σ-holes to facilitate bond formation. These Lewis acid molecules contain an F substituent whose electronegativity is strong enough to foster the appearance of a σ -hole on the atom to which it is bound. Not only monofluorinated molecules were considered but also perfluorinated to cover the full range of substituent effect. The base atoms were all drawn from the pnicogen family as representing good electron donors. The size was varied from N, which is the one that appears in most previous studies, up to larger P, As, and Sb. The first series of bases were purely hydrogenated ZH₃, where Z represents the pnicogen atom. Since many of the relevant systems of interest would place the Z within the context of a larger unit, bound to several C atoms, the study was expanded to include the trimethyl ZMe3 series of bases.

Methods

Quantum chemical calculations were carried out with the aid of the Gaussian 16⁷⁴ program. The M06-2X functional⁷⁵ was applied in the context of the def2-TZVP basis set which includes a triple- ζ foundation. This functional has been repeatedly assessed to be one of the most accurate for interactions such as those considered here. 76-83 Geometries were fully optimized,

and verified as true minima by the lack of any imaginary vibrational frequencies. The interaction energy E_{int} is formulated as the difference between the energy of each complex and the sum of the energies of the two subunits in the geometry they adopt within the complex. $E_{\rm int}$ was corrected for basis set superposition error by the counterpoise procedure.84 The Multiwfn program⁸⁵ located the maxima and minima of the molecular electrostatic potential (MEP) on the $\rho = 0.001$ a.u. isodensity surface of each monomer. NMR chemical shielding calculations applied the GIAO approximation. 86,87 A pseudopotential was not considered adequate for purposes of assessing the shielding of Sb as this approach would not offer sufficient flexibility to the inner electrons near the nucleus. Consequently, the NMR calculations of the systems containing SbH3 employed the all-electron Sapporo-DKH3-TZP-2012 basis set88,89 which was calibrated to include certain relativistic effects.

Results

Monomer potentials

With regard to the molecular electrostatic potential (MEP) of each monomer, each of the Lewis acids contains a positive region which interacts favorably with the negative area on the base. This MEP is illustrated in Fig. 1 for each acid monomer where the blue region to the right of the central atom represents the σ -hole that can interact with a base. The magnitude of this positive region is quantified as the maximum of the MEP on the ρ = 0.001 a.u. isodensity surface, V_{max} , which is displayed in Table 1. The most intense maximum of 69 kcal mol occurs on the H of the HF molecule. The values for the various other acids all lie in the range between 41 and 53 kcal mol⁻¹. In the case of the perfluorinated acids in the first row of diagrams in Fig. 1, the σ -hole is most intense on Ge, followed in order by Br, Se, and then As. (The lighter blue color surrounding Ge, as compared to the As, Se, etc. atoms is due to its larger vdW radius which is taken as the basis of the surfaces in Fig. 1.) Removing one or more F atoms to reach the monofluorinated

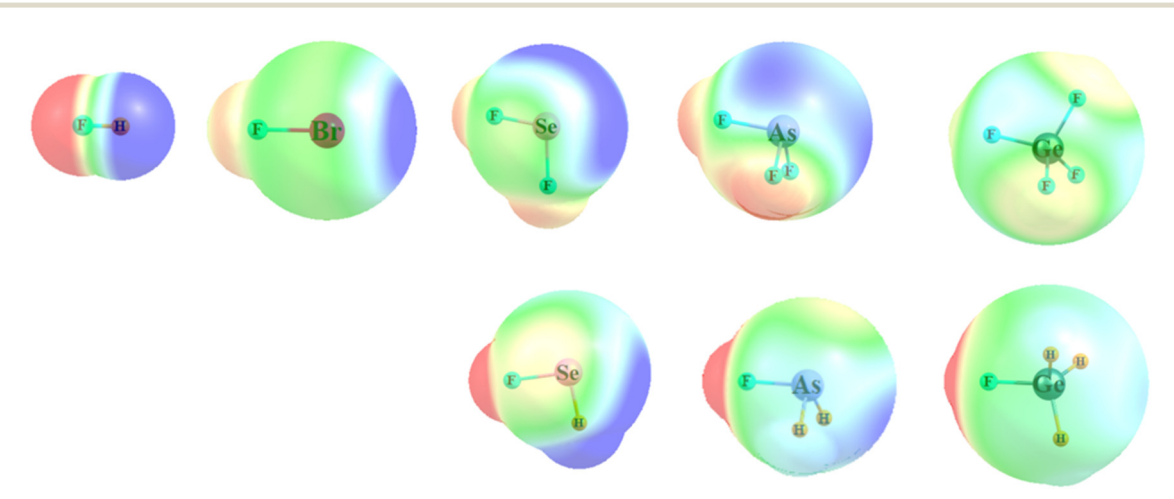


Fig. 1 Molecular electrostatic potential (MEP) surrounding each of the Lewis acid molecules. Surface represents 1.5 × vdW radius. Blue color indicates +25 kcal mol⁻¹, and red represents -20 kcal mol⁻¹.

Table 1 V_{max} of acids, kcal mol^{-1}

FH	FBr	F ₂ Se	F ₃ As	F ₄ Ge	
68.7	50.3	46.2	40.7	52.5	
		FHSe	FH ₂ As	FH ₃ Ge	
		47.0	42.0	41.8	

acids has a mixed effect. Although the removal of three F atoms from GeF $_4$ drops $V_{\rm max}$ significantly, such F to H substitutions exert only a marginal influence for Se and As, actually raising it a small amount. But in a larger view, all of these acids contain a healthy positive region, ready to attract a negative base.

The minimum of the MEP on each base coincides with its C_3 symmetry axis, *i.e.* the lone pair. This minimum is evaluated, again on the $\rho=0.001$ a.u. isodensity surface, and is reported in Table 2 as V_{\min} . Whether ZH $_3$ or ZMe $_3$ (where Z represents the central pnicogen atom), V_{\min} is largest in magnitude for N, dropping along with the size of the Z atom. With the exception of N, the replacement of the three H atoms on ZH $_3$ by methyl intensifies this minimum by a substantial amount. NH $_3$ is the outlier here, in that V_{\min} is smaller for NMe $_3$ than for NH $_3$. This less negative quantity may be due in part to the precise location of the minimum on the $\rho=0.001$ a.u. surface. This minimum

Table 2 V_{\min} of bases, kcal \mod^{-1}

NH ₃	PH_3	AsH_3	SbH_3
-40.1	-16.3	-12.5	-7.41
NMe ₃	PMe_3	$AsMe_3$	SbMe ₃
-32.0	-26.9	-22.4	-16.7

lies closer to the N in NMe_3 than in NH_3 by some 0.046 Å. The shorter distance places the point of reference closer to the highly positively charged N nucleus, thereby making the potential less negative. The weakening trend associated with the heavier Z atom casts into question whether Sb can serve as an effective nucleophilic atom.

Energetics

Upon pairing each Lewis acid with a base, the resulting dyad places the base Z atom roughly along the extension of the F-A covalent bond where A represents the central atom of the acid. Several representative structures are depicted in Fig. 2; coordinates of all optimized structures are contained in the ESI.† The interaction energy of each acid-base dyad combination is listed in Table 3, where it may be seen to scan a wide range from less than 3 all the way up to 49 kcal mol⁻¹. There are certain easily distinguished patterns that characterize these complexes. E_{int} is largest for the N-bases, then takes a big step down to P, after which there is a slower decline as the base atom grows larger. Adding the three methyl groups to the base produces a sizable rise in the interaction energy, even for N where V_{\min} is smaller in magnitude for NMe3 than for NH3. In most cases, the halogen bond (XB) with FBr is the strongest type, followed by the chalcogen bond (YB) with Se. In many but not all cases, the YB and tetrel bond (TB) are slightly weaker. An obvious exception occurs for some of the TBs with Ge that are very strong indeed, particularly with the methylated bases. The F₄Ge·NH₃ interaction energy is 37 kcal mol⁻¹, and nearly 50 kcal mol⁻¹ with NMe₃. F₄Ge forms very strong TBs with heavier methylated bases PMe₃ and AsMe₃, both over 30 kcal mol⁻¹.

With regard to the fluorination level of the acid, recall from Table 1 that the reduction to monofluorination of Se and As yielded a small increase in V_{max} , while this quantity was

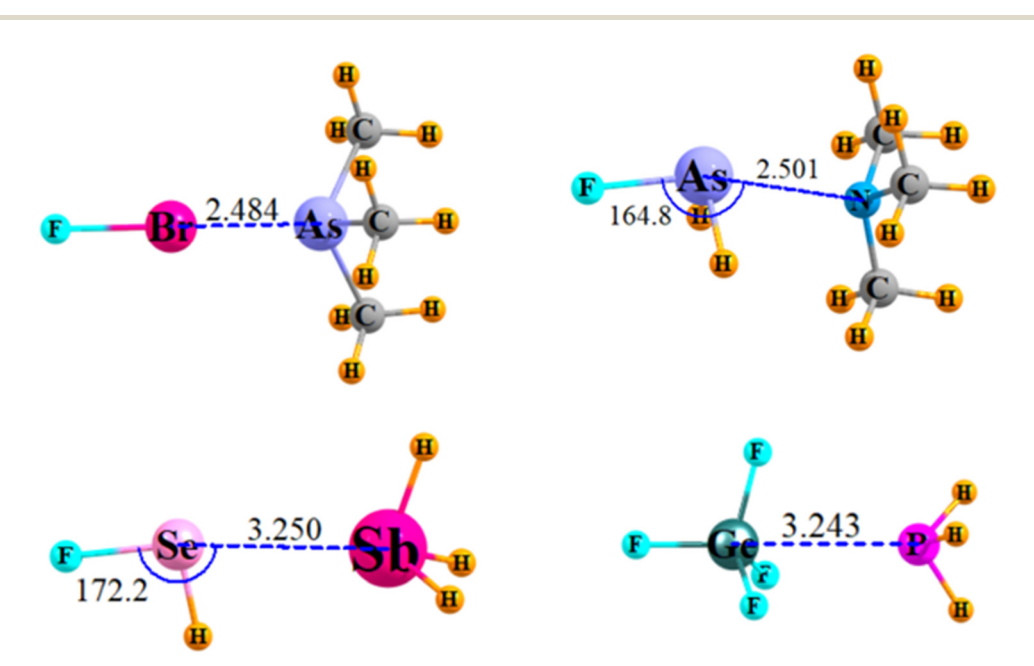


Fig. 2 Optimized geometries of several sample dyads. Distances in Å, angles in degs.

Paper PCCP

Table 3 Interaction energies $-E_{int}$ (kcal mol⁻¹) for acid-base complexes

Perfluor	D										
	FH	FBr	F ₂ Se	F_3As	F ₄ Ge		FH	FBr	F ₂ Se	F_3As	F ₄ Ge
NH ₃	13.81	15.12	13.24	10.24	36.80	NMe ₃	16.72	23.71	21.38	15.83	49.42
PH_3	5.08	15.08	5.95	3.72	6.30	PMe_3	9.04	40.42	23.95	8.42	43.99
AsH_3	4.24	11.59	5.00	3.09	4.71	$AsMe_3$	7.36	29.49	13.46	6.67	32.56
SbH_3	3.29	11.00	4.30	2.64	3.57	SbMe ₃	5.48	23.76	9.86	4.98	8.13
Monoflu	oro										
	FH	FBr	FHSe	$\mathrm{FH}_2\mathrm{As}$	FH₃Ge		FH	FBr	FHSe	$\mathrm{FH}_2\mathrm{As}$	FH ₃ Ge
NH ₃	13.81	15.12	11.45	8.77	8.64	NMe ₃	16.72	23.71	17.81	13.03	14.34
PH_3	5.08	15.08	7.17	4.55	3.51	PMe ₃	9.04	40.42	20.63	9.03	6.28
AsH ₃	4.24	11.59	5.92	4.12	3.06	AsMe ₃	7.36	29.49	13.99	6.95	5.08
SbH_3	3.29	11.00	5.44	3.64	2.56	$SbMe_3$	5.48	23.76	10.22	5.42	3.81

Table 4 Deformation energy E_{def} (kcal mol^{-1}) involved in geometry changes within each subunit during complexation

Perfluoro)										
	FH	FBr	F_2Se	F_3As	F_4Ge		FH	FBr	F_2Se	F_3As	F_4Ge
NH ₃	0.80	1.18	1.35	0.82	16.21	NMe ₃	2.15	2.71	2.96	1.96	23.18
PH_3	0.27	2.97	0.67	0.80	1.86	PMe_3	0.59	14.62	9.10	0.94	27.09
AsH_3	0.19	2.77	0.41	0.10	0.99	$AsMe_3$	0.31	10.48	3.80	0.55	22.36
SbH_3	0.15	2.62	0.31	0.10	0.59	$SbMe_3$	0.28	8.04	2.42	0.31	3.23
Monoflu	oro										
	FH	FBr	FHSe	$\mathrm{FH}_2\mathrm{As}$	FH_3Ge		FH	FBr	FHSe	$\mathrm{FH}_2\mathrm{As}$	FH₃G€
NH ₃	0.80	1.18	0.57	0.29	0.02	NMe ₃	2.15	2.71	1.63	0.89	2.75
PH_3	0.27	2.97	0.73	0.13	0.12	PMe_3	0.59	14.62	5.37	0.84	0.46
AsH_3	0.19	2.77	0.39	0.10	0.08	$AsMe_3$	0.31	10.48	2.92	0.44	0.29
SbH_3	0.15	2.62	0.25	0.09	0.06	SbMe ₃	0.28	8.04	1.62	0.20	0.10

diminished for Ge. This pattern is partially predictive of the energetics. First with respect to the unmethylated bases, the removal of an F atom from F_2Se and F_3As does raise the interaction energy (with the exception of the opposite trend for NH_3), while FH_3Ge engages in a weaker tetrel bond than does F_4Ge , all consistent with V_{max} trends. When the base is trimethylated, these patterns largely remain, except for an obvious apparent anomaly for the Ge tetrel bonds in the last column of Table 3, which drop drastically when three of the F atoms of GeF_4 are replaced by H.

 $E_{\rm int}$ represents the interaction between the two subunits after they have adopted their geometries within the fully optimized dyad. The deformation required to morph from the optimized structure of the monomer to that within the dimer can be significant. As one example, the fully optimized GeF₄ monomer is fully tetrahedral with a r(GeF) bond length of 1.690 Å. However, when complexed with NMe₃, the $\theta(\text{F-Ge-F})$ angle involving the F lying opposite the N is reduced by 14° to 95.3°, as the molecule converts partially toward a trigonal bipyramid shape, and the r(GeF) bondlength stretches by 0.034 Å to 1.724 Å. This particular deformation raises the energy of the GeF₄ molecule by 21.7 kcal mol⁻¹. When combined with a smaller distortion within the NMe₃ base, the total deformation energy of this complex is equal to 23.18 kcal mol⁻¹. (Deformation energies of both the acid and base within each dyad are reported

in Table S1, ESI†). This quantity, along with the deformation energies of the other complexes, is displayed in Table 4. The actual energy change in going from a fully separated acid + base pair to the complex, ΔE , would then be the interaction energy minus this deformation energy $E_{\rm def}$. Again taking GeF₄·NMe₃ as the example, this reaction energy would be 49.42–23.18, or 26.24 kcal mol⁻¹. This difference still represents a strongly bound structure, but only half as much as might be deduced from the interaction energy alone.

Perusal of Table 4 suggests $GeF_4 \cdot NMe_3$ is not the norm, as most deformation energies are rather small, so the interaction energies are not far off the mark as a measure of ΔE . The exceptions that involve substantial $E_{\rm def}$ are the complexes of GeF_4 with NH_3 , NMe_3 , PMe_3 , and $AsMe_3$, all exceeding 20 kcal mol^{-1} . Other substantial deformations occur for the halogen bonded complexes of FBr with PMe_3 and $AsMe_3$, with $E_{\rm def}$ between 10 and 15 kcal mol^{-1} .

Geometries and NMR spectra

One would normally expect a strong relationship in that stronger noncovalent bonds ought to be associated with a shorter intermolecular distance. These distances are listed in Table S2 (ESI†) for each of the dyads. It is difficult to relate these distances themselves directly to the energetics, since there are different size atoms from one pair to the next.

PCCP Paper

Table 5 Normalized intermolecular distances, expressed as ratio $R/\sum r_{vdW}$

Perfluor)										
	FH	FBr	F ₂ Se	F_3As	F ₄ Ge		FH	FBr	F ₂ Se	F ₃ As	F ₄ Ge
NH ₃	0.587	0.671	0.704	0.750	0.537	NMe ₃	0.550	0.639	0.662	0.694	0.536
PH_3	0.760	0.665	0.822	0.909	0.774	PMe_3	0.722	0.614	0.677	0.841	0.589
AsH_3	0.803	0.713	0.876	0.949	0.822	$AsMe_3$	0.772	0.664	0.763	0.894	0.630
SbH_3	0.727	0.650	0.799	0.859	0.767	$SbMe_3$	0.710	0.618	0.712	0.830	0.713
Monoflu	oro										
	FH	FBr	FHSe	$\mathrm{FH}_2\mathrm{As}$	FH₃Ge		FH	FBr	FHSe	$\mathrm{FH}_2\mathrm{As}$	FH ₃ Ge
NH ₃	0.587	0.671	0.726	0.770	0.691	NMe ₃	0.550	0.639	0.675	0.706	0.625
PH_3	0.760	0.665	0.772	0.871	0.824	PMe ₃	0.722	0.614	0.676	0.773	0.780
AsH ₃	0.803	0.713	0.842	0.902	0.855	AsMe ₃	0.772	0.664	0.735	0.833	0.818
SbH_3	0.727	0.650	0.758	0.817	0.788	SbMe ₃	0.710	0.618	0.689	0.784	0.768

For example, as one moves down any column the electron acceptor atom is growing larger, which would of course tend to elongate the intermolecular distance, thus masking changes induced by stronger or weaker bonding. It perhaps makes more sense to normalize each of these distances by dividing it by the sum of vdW radii of the two atoms involved. This quotient, is commonly assessed in crystal studies where it is sometimes referred to as contact distance, and would better express the penetration of each atom into the electron cloud of its partner, where a smaller ratio would be indicative of a stronger bond.

These normalized distances are listed in Table 5 where clearer trends than those seen in Table S2 (ESI†) emerge immediately, some of which parallel the energetic trends in Table 3. In most cases, the N base approaches the acid more closely than do the heavier base atoms. It is the heaviest Sb that is next in this list, followed by P and then As. With respect to the acidic electron acceptor atom, in most cases, this follows the order Br < Ge < Se < As. The addition of methyl groups to the base shortens this distance, in line with the strengthening energetics. The exceptions to these trends generally coincide with the surprisingly large TB energies for some of the Ge acids, each of which results in a particularly close distance of approach.

Due in large part to the transfer of a certain amount of density from the base to the $\sigma^*(AF)$ antibonding orbital of the acid, the associated A-F bond tends to stretch. This elongation

is quantified in Table 6 for each of the acid-base dyads. The trends generally reflect a reduced stretch as the base atom becomes heavier, but the XBs with FBr are an exception in that NH₃ induces the smallest stretch. In general, the XBs cause the largest bond stretch, followed by the YB, and then pnicogen bond (ZB) and TB. Removing the F atoms from the acid other than the one that causes the σ -hole with which the base reacts usually raises the degree of A-F stretch.

Several earlier works have suggested that within the context of σ-hole noncovalent bonds, the property of the NMR spectrum which is most heavily connected to the bond energy is the change in the chemical shielding of the base atom that arises upon complexation. This quantity is thus reported in Table 7 for each of the acid-base complexes and reflects certain patterns. In the first place, and perhaps most important, the shielding changes on these base atoms are quite substantial. With few exceptions, the shielding diminishes upon forming the noncovalent bond, so the NMR spectra ought to serve as a signpost of such bond formation. This sort of change is verified by recent measurements⁹⁰ that noted a drop in the experimental electron density surrounding an electrondonor N atom when participating in XBs, and that the magnitude of this drop correlates with XB strength.

Whether N, P, As, or Sb, the largest deshielding occurs within the XB with FBr, followed by the YB, with HB, TB, and ZB taking up the rear. This trend more or less conforms to the

Table 6 Change in internal Λ – E hand length $(\mathring{\Lambda})$ upon forming complex

Perfluoro											
	FH	FBr	F_2Se	F_3As	F_4Ge		FH	FBr	F_2Se	F_3As	F_4Ge
NH ₃	0.0349	0.0598	0.0385	0.0218	0.0282	NMe ₃	0.0559	0.0870	0.0564	0.0322	0.0342
PH_3	0.0105	0.0978	0.0200	0.0062	0.0083	PMe_3	0.0209	0.2065	0.0857	0.0170	0.0322
AsH_3	0.0086	0.0757	0.0150	0.0059	0.0061	$AsMe_3$	0.0154	0.1644	0.0546	0.0111	0.0299
SbH_3	0.0073	0.0786	0.0126	0.0042	0.0043	$SbMe_3$	0.0115	0.1466	0.0380	0.0059	0.0111
Monoflu	ioro										
	FH	FBr	FHSe	FH_2As	FH ₃ Ge		FH	FBr	FHSe	FH_2As	FH ₃ Ge
NH ₃	0.0349	0.0598	0.0395	0.0270	0.0228	NMe ₃	0.0559	0.0870	0.0610	0.0395	0.0327
PH_3	0.0105	0.0978	0.0354	0.0128	0.0083	PMe_3	0.0209	0.2065	0.1080	0.0332	0.0155
AsH_3	0.0086	0.0757	0.0220	0.0109	0.0069	$AsMe_3$	0.0154	0.1644	0.0755	0.0231	0.0116
SbH_3	0.0073	0.0786	0.0206	0.0090	0.0053	SbMe ₃	0.0115	0.1466	0.0568	0.0166	0.0080

Paper PCCP

Table 7 Change in base atom isotropic shielding (ppm) upon forming complex

Perfluoro												
	FH	FBr	F ₂ Se	F_3As	F ₄ Ge		FH	FBr	F_2Se	F_3As	F ₄ Ge	
$\overline{\mathrm{NH_3}}$	-14.6	-22.0	-32.6	-32.9	-45.1	NMe ₃	-8.6	-28.6	-31.3	-22.8	-38.4	
PH_3	-20.5	-100.0	-43.6	-22.5	-23.9	PMe_3	-5.4	-80.9	-66.2	-10.2	-36.6	
AsH_3	-16.5	-149.4	-54.5	-25.7	-25.3	$AsMe_3$	-2.5	-156.9	-101.6	-17.4	-67.3	
SbH_3	-46.1	-305.1	-103.7	-30.5	-40.5	$SbMe_3$	+8.4	-219.7	-91.4	+0.9	+26.2	

Monofluoro											
	FH	FBr	FHSe	FH_2As	FH_3Ge		FH	FBr	FHSe	FH_2As	FH ₃ Ge
$\overline{NH_3}$	-14.6	-22.0	-15.3	-12.3	-18.3	NMe ₃	-8.6	-28.6	-19.1	-19.0	-10.5
PH_3	-20.5	-100.0	-48.3	-18.2	-13.0	PMe_3	-5.4	-80.9	-54.0	-17.7	-3.2
AsH_3	-16.5	-149.4	-54.8	-22.5	-9.7	$AsMe_3$	-2.5	-156.9	-96.3	-25.4	-4.9
SbH_3	-46.1	-305.1	-138.2	-45.5	-18.5	SbMe ₃	+8.4	-219.7	-136.3	-6.4	-6.5

energetic data in Table 3. The effect of adding methyl groups to the base atom has a variable effect, sometime less and sometimes more deshielding. There is a general trend for the deshielding to rise along with the size of the base atom, but again not without exceptions. This pattern is contrary to the interaction energies which are clearly largest for N. As a bottom line, the connections between these shielding changes and the interaction energy are tenuous.

Conclusions

Not only can the heavier pnicogen atoms act as electron donor within the context of HBs, but the same capability extends to the full variety of σ -hole noncovalent bonds. In fact, the latter sorts of bonds are comparable in strength to the HB, exceeding it in some cases. The halogen bond, for example, is particularly strong, in some cases with 3 to 4 times the interaction energy of the corresponding HB. In most but not all cases, N forms the strongest bonds, with the heavier pnicogens not far behind, weakening only slowly as the Z atom grows larger. Certain of the tetrel bonds to F₄Ge have a particularly large interaction energy, but this comes at the expense of a large deformation energy of this Lewis acid molecule. When the Z atom is trimethylated, simulating the situation within many molecules where it is bonded to three C atoms, the noncovalent bonds are quite strong, some with interaction energies exceeding 40 kcal mol⁻¹. The optimized intermolecular distances are quite a bit smaller than the sum of atomic vdW radii, which should facilitate identification of these bonds via diffraction data of crystals. NMR spectroscopy would also be a useful tool as the noncovalent bond formation induces a substantial drop in the NMR shielding of the base atom.

Conflicts of interest

The authors declare no conflict of interest.

Acknowledgements

This material is based upon work supported by the National Science Foundation under Grant No. 1954310.

References

- 1 G. C. Pimentel and A. L. McClellan, *The Hydrogen Bond*, Freeman, San Francisco, 1960.
- 2 W. C. Hamilton and J. A. Ibers, Hydrogen Bonding in Solids, W. A. Benjamin, New York, 1968.
- 3 M. D. Joesten and L. J. Schaad, *Hydrogen Bonding*, Marcel Dekker, New York, 1974.
- 4 M. V. Vener and S. Scheiner, *J. Phys. Chem.*, 1995, **99**, 642–649.
- 5 P. Schuster, G. Zundel and C. Sandorfy, *The Hydrogen Bond. Recent Developments in Theory and Experiments*, North-Holland Publishing Co., Amsterdam, 1976.
- 6 M. M. Szczesniak and S. Scheiner, J. Chem. Phys., 1982, 77, 4586–4593.
- 7 G. A. Jeffrey and W. Saenger, *Hydrogen Bonding in Biological Structures*, Springer-Verlag, Berlin, 1991.
- 8 S. Scheiner, *Hydrogen Bonding: A Theoretical Perspective*, Oxford University Press, New York, 1997.
- 9 G. Gilli and P. Gilli, *The Nature of the Hydrogen Bond*, Oxford University Press, Oxford, UK, 2009.
- 10 M. M. Szczesniak, S. Scheiner and Y. Bouteiller, J. Chem. Phys., 1984, 81, 5024–5030.
- 11 S. M. Cybulski and S. Scheiner, *Chem. Phys. Lett.*, 1990, **166**, 57–64.
- 12 E. A. Hillenbrand and S. Scheiner, J. Am. Chem. Soc., 1984, 106, 6266–6273.
- E. Arunan, G. R. Desiraju, R. A. Klein, J. Sadlej, S. Scheiner,
 I. Alkorta, D. C. Clary, R. H. Crabtree, J. J. Dannenberg,
 P. Hobza, H. G. Kjaergaard, A. C. Legon, B. Mennucci and
 D. J. Nesbitt, *Pure Appl. Chem.*, 2011, 83, 1637–1641.
- 14 L. T. Maltz, L. C. Wilkins and F. P. Gabbaï, *Chem. Commun.*, 2022, 58, 9650–9653.
- 15 S. Gholami, M. Aarabi and S. J. Grabowski, *J. Phys. Chem. A*, 2021, 125, 1526–1539.
- 16 K. K. Mishra, S. K. Singh, S. Kumar, G. Singh, B. Sarkar, M. S. Madhusudhan and A. Das, *J. Phys. Chem. A*, 2019, 123, 5995–6002.
- 17 H. Schmidbaur, Angew. Chem., Int. Ed., 2019, 58, 5806-5809.
- 18 V. R. Mundlapati, S. Gautam, D. K. Sahoo, A. Ghosh and H. S. Biswal, *J. Phys. Chem. Lett.*, 2017, **8**, 4573–4579.

PCCP Paper

- 19 S. J. Grabowski and F. Ruipérez, Chem. Phys. Chem., 2017, 18, 2409-2417.
- 20 M. A. Trachsel, P. Ottiger, H.-M. Frey, C. Pfaffen, A. Bihlmeier, W. Klopper and S. Leutwyler, *J. Phys. Chem. B*, 2015, **119**, 7778–7790.
- 21 P. Banerjee and T. Chakraborty, *J. Phys. Chem. A*, 2014, **118**, 7074–7084.
- 22 A. E. Aliev, J. R. T. Arendorf, I. Pavlakos, R. B. Moreno, M. J. Porter, H. S. Rzepa and W. B. Motherwell, *Angew. Chem.*, *Int. Ed.*, 2015, 54, 551–555.
- 23 S. J. Grabowski, Chem. Phys. Chem., 2019, 20, 565-574.
- 24 I. Alkorta, C. Martín-Fernández, M. M. Montero-Campillo and J. Elguero, *J. Phys. Chem. A*, 2018, **122**, 1472–1478.
- 25 V. V. Karpov, A. M. Puzyk, P. M. Tolstoy and E. Y. Tupikina, J. Comput. Chem., 2021, 42, 2014–2023.
- 26 K. K. Mishra, K. Borish, G. Singh, P. Panwaria, S. Metya, M. S. Madhusudhan and A. Das, J. Phys. Chem. Lett., 2021, 12, 1228–1235.
- 27 S. Scheiner, CrystEngComm, 2021, 23, 6821-6837.
- 28 A. Chand, D. K. Sahoo, A. Rana, S. Jena and H. S. Biswal, *Acc. Chem. Res.*, 2020, **53**, 1580–1592.
- 29 A. Das, P. K. Mandal, F. J. Lovas, C. Medcraft, N. R. Walker and E. Arunan, *Angew. Chem., Int. Ed.*, 2018, 57, 15199–15203.
- 30 D. F. Mertsalov, R. M. Gomila, V. P. Zaytsev, M. S. Grigoriev, E. V. Nikitina, F. I. Zubkov and A. Frontera, *Crystals*, 2021, 11, 1406.
- 31 J. E. Del Bene, I. Alkorta and J. Elguero, *Chem. Phys. Lett.*, 2020, **761**, 137916.
- 32 M. Palusiak and S. J. Grabowski, *Struct. Chem.*, 2008, **19**, 5–11.
- 33 S. J. Grabowski, J. Phys. Chem. A, 2011, 115, 12340-12347.
- 34 S. Scheiner and S. Hunter, *Chem. Phys. Chem.*, 2022, 23, e202200011.
- 35 J. S. Murray and P. Politzer, *Chem. Phys. Chem.*, 2021, 22, 1201–1207.
- 36 A. V. Cunha, R. W. A. Havenith, J. van Gog, F. De Vleeschouwer, F. De Proft and W. Herrebout, *Molecules*, 2023, **28**, 772.
- 37 L. M. Azofra and S. Scheiner, *J. Chem. Phys.*, 2015, 142, 034307.
- 38 A. Bauzá and A. Frontera, Theor. Chem. Acc., 2017, 136, 37.
- 39 G. Cavallo, P. Metrangolo, R. Milani, T. Pilati, A. Priimagi, G. Resnati and G. Terraneo, *Chem. Rev.*, 2016, **116**, 2478–2601.
- 40 S. Scheiner, CrystEngComm, 2013, 15, 3119-3124.
- 41 T. Clark, M. Hennemann, J. S. Murray and P. Politzer, *J. Mol. Model.*, 2007, **13**, 291–296.
- 42 A. J. Taylor, A. Docker and P. D. Beer, *Chem. Asian J.*, 2023, **18**, e202201170.
- 43 C. B. Aakeroy, D. L. Bryce, G. R. Desiraju, A. Frontera, A. C. Legon, F. Nicotra, K. Rissanen, S. Scheiner, G. Terraneo, P. Metrangolo and G. Resnati, *Pure Appl. Chem.*, 2019, 91, 1889.
- 44 G. R. Desiraju and V. Nalini, *J. Mater. Chem.*, 1991, 1, 201–203.
- 45 M. Iwaoka and S. Tomoda, J. Am. Chem. Soc., 1994, 116, 2557–2561.

46 R. J. Fick, G. M. Kroner, B. Nepal, R. Magnani, S. Horowitz, R. L. Houtz, S. Scheiner and R. C. Trievel, ACS Chem. Biol., 2016, 11, 748–754.

- 47 J. Fanfrlík, A. Přáda, Z. Padělková, A. Pecina, J. Macháček, M. Lepšík, J. Holub, A. Růžička, D. Hnyk and P. Hobza, *Angew. Chem., Int. Ed.*, 2014, **53**, 10139–10142.
- 48 A. C. Legon, Phys. Chem. Chem. Phys., 2017, 19, 14884-14896.
- 49 C. Trujillo, I. Rozas, J. Elguero, I. Alkorta and G. Sánchez-Sanz, *Phys. Chem. Chem. Phys.*, 2019, **21**, 23645–23650.
- 50 S. Scheiner and J. Lu, Chem. Eur. J., 2018, 24, 8167-8177.
- 51 O. Carugo, G. Resnati and P. Metrangolo, *ACS Chem. Biol.*, 2021, **16**, 1622–1627.
- 52 H. S. Biswal, A. K. Sahu, B. Galmés, A. Frontera and D. Chopra, *ChemBioChem*, 2022, 23, e202100498.
- 53 K. T. Mahmudov, A. V. Gurbanov, V. A. Aliyeva, M. F. C. Guedes da Silva, G. Resnati and A. J. L. Pombeiro, *Coord. Chem. Rev.*, 2022, **464**, 214556.
- 54 A. Bauzá, D. Quiñonero, P. M. Deyà and A. Frontera, *Phys. Chem. Chem. Phys.*, 2012, **14**, 14061–14066.
- 55 Q.-Z. Li, R. Li, X.-F. Liu, W.-Z. Li and J.-B. Cheng, Chem. Phys. Chem., 2012, 13, 1205–1212.
- 56 U. Adhikari and S. Scheiner, *Chem. Phys. Lett.*, 2012, **536**, 30–33.
- 57 D. Setiawan, E. Kraka and D. Cremer, J. Phys. Chem. A, 2015, 119, 1642–1656.
- 58 M. D. Esrafili, F. Mohammadian-Sabet and E. Vessally, *Mol. Phys.*, 2016, **114**, 2115–2122.
- 59 S. Sarkar, M. S. Pavan and T. N. Guru Row, *Phys. Chem. Chem. Phys.*, 2015, 17, 2330-2334.
- 60 D. Mani and E. Arunan, Phys. Chem. Chem. Phys., 2013, 15, 14377–14383.
- 61 P. R. Varadwaj, A. Varadwaj, H. M. Marques and K. Yamashita, *CrystEngComm*, 2023, **25**, 1411–1423.
- 62 S. A. Southern, T. Nag, V. Kumar, M. Triglav, K. Levin and D. L. Bryce, *J. Phys. Chem. C*, 2022, **126**, 851–865.
- 63 S. A. C. McDowell, N. Liu and Q. Li, *Mol. Phys.*, 2022, **120**, e2111374.
- 64 S. J. Grabowski, Crystals, 2022, 12, 112.
- 65 A. Grabarz, M. Michalczyk, W. Zierkiewicz and S. Scheiner, *Chem. Phys. Chem.*, 2020, 21, 1934–1944.
- 66 W. Zierkiewicz, M. Michalczyk, R. Wysokiński and S. Scheiner, *Molecules*, 2019, 24, 376.
- 67 C. Trujillo, I. Alkorta, J. Elguero and G. Sánchez-Sanz, *Molecules*, 2019, **24**, 308.
- 68 V. d P. N. Nziko and S. Scheiner, *Phys. Chem. Chem. Phys.*, 2016, **18**, 3581–3590.
- 69 K. Lisac, F. Topić, M. Arhangelskis, S. Cepić, P. A. Julien, C. W. Nickels, A. J. Morris, T. Friščić and D. Cinčić, *Nat. Commun.*, 2019, 10, 61.
- 70 Y. Xu, J. Huang, B. Gabidullin and D. L. Bryce, *Chem. Commun.*, 2018, 54, 11041–11043.
- 71 D. N. Zheng, P. M. J. Szell, S. Khiri, J. S. Ovens and D. L. Bryce, *Acta Crystallogr., Sect. B: Struct. Sci., Cryst. Eng. Mater.*, 2022, **78**, 557–563.
- 72 A. M. Siegfried, H. D. Arman, K. Kobra, K. Liu, A. J. Peloquin, C. D. McMillen, T. Hanks and W. T. Pennington, Cryst. Growth Des., 2020, 20, 7460–7469.

Paper PCCP

73 S. Liyanage, J. S. Ovens, S. Scheiner and D. L. Bryce, Chem. Commun., 2023, 59, 9001-9004.

- 74 M. J. Frisch, G. W. Trucks, H. B. Schlegel, G. E. Scuseria, M. A. Robb, J. R. Cheeseman, G. Scalmani, V. Barone, G. A. Petersson, H. Nakatsuji, X. Li, M. Caricato, A. V. Marenich, J. Bloino, B. G. Janesko, R. Gomperts, B. Mennucci, H. P. Hratchian, J. V. Ortiz, A. F. Izmaylov, J. L. Sonnenberg, D. Williams-Young, F. Ding, F. Lipparini, F. Egidi, J. Goings, B. Peng, A. Petrone, T. Henderson, D. Ranasinghe, V. G. Zakrzewski, J. Gao, N. Rega, G. Zheng, W. Liang, M. Hada, M. Ehara, K. Toyota, R. Fukuda, J. Hasegawa, M. Ishida, T. Nakajima, Y. Honda, O. Kitao, H. Nakai, T. Vreven, K. Throssell, J. A. Montgomery Jr, J. E. Peralta, F. Ogliaro, M. J. Bearpark, J. J. Heyd, E. N. Brothers, K. N. Kudin, V. N. Staroverov, T. A. Keith, R. Kobayashi, J. Normand, K. Raghavachari, A. P. Rendell, J. C. Burant, S. S. Iyengar, J. Tomasi, M. Cossi, J. M. Millam, M. Klene, C. Adamo, R. Cammi, J. W. Ochterski, R. L. Martin, K. Morokuma, O. Farkas, J. B. Foresman and D. J. Fox, Gaussian-16, Wallingford, CT, 2016.
- 75 Y. Zhao and D. G. Truhlar, Theor. Chem. Acc., 2008, 120, 215-241
- 76 B. S. D. R. Vamhindi and A. Karton, Chem. Phys., 2017, 493, 12-19.

- 77 R. Podeszwa and K. Szalewicz, J. Chem. Phys., 2012, 136, 161102.
- 78 S. Karthikeyan, V. Ramanathan and B. K. Mishra, J. Phys. Chem. A, 2013, 117, 6687-6694.
- 79 M. Majumder, B. K. Mishra and N. Sathyamurthy, Chem. Phys., 2013, 557, 59-65.
- 80 M. A. Vincent and I. H. Hillier, Phys. Chem. Chem. Phys., 2011, 13, 4388-4392.
- 81 A. D. Boese, Chem. Phys. Chem., 2015, 16, 978-985.
- 82 M. Walker, A. J. A. Harvey, A. Sen and C. E. H. Dessent, J. Phys. Chem. A, 2013, 117, 12590-12600.
- 83 L. F. Molnar, X. He, B. Wang and K. M. Merz, J. Chem. Phys., 2009, 131, 065102.
- 84 S. F. Boys and F. Bernardi, Mol. Phys., 1970, 19, 553-566.
- 85 T. Lu and F. Chen, J. Comput. Chem., 2012, 33, 580-592.
- 86 R. Ditchfield, Chem. Phys. Lett., 1976, 40, 53-56.
- 87 I. Alkorta and J. Elguero, Struct. Chem., 1998, 9, 187-202.
- 88 T. Noro, M. Sekiya and T. Koga, Theor. Chem. Acc., 2012, **131**, 1124.
- 89 T. Noro, M. Sekiya and T. Koga, Theor. Chem. Acc., 2013, **132**, 1363.
- 90 F. Otte, J. Kleinheider, B. Grabe, W. Hiller, F. Busse, R. Wang, N. M. Kreienborg, C. Merten, U. Englert and C. Strohmann, ACS Omega, 2023, 8, 21531–21539.